PROCEEDINGS, 51st Workshop on Geothermal Reservoir Engineering
Stanford University, Stanford, California, February 9-11, 2026
SGP-TR-230

Advances in Tensor Strainmeters for Geothermal Reservoir Applications

Josh Parris[1], Scott DeWolf [1, 3], Leonid Germanovich, Adam J. Hawkins[1], Eduardo Andres Paba Vega[2], Catalin Teodoriu[2], Lawrence C. Murdoch[1]

[1]School of Civil and Environmental Engineering and Earth Sciences, College of Engineering, Computing and Applied Sciences, Clemson University, Clemson, SC, USA

[2]Mewbourne School of Petroleum and Geological Engineering (MPGE), The University of Oklahoma, Norman, OK, USA

[3]Tensora Inc., Brooklyn, NY, USA

Keywords: Enhanced geothermal energy (EGS), strainmeter, strain, deformation, reservoir monitoring, Utah FORGE

ABSTRACT

Direct measurement of deformation in geothermal reservoirs can provide valuable constraints on stimulation and heat extraction processes. It is feasible to characterize deformation with borehole tensor strainmeters, which can measure multiple components of strain at high resolution, but currently available instruments are limited to ambient temperatures. We have developed a tensor strainmeter for geothermal reservoir conditions. It is a thin sleeve containing optical fibers that is clamped around a casing, and we have conducted a suite of experiments to demonstrate performance in the laboratory. One experiment consisted of deploying a sleeve strainmeter on a steel pipe that was subjected to periodic transverse loads while heated to 225–275 °C for nine months. The strainmeter measured strain responses of up to 30 με each time the transverse load was applied. The magnitude at each sensor varied slightly during the experiment, but there was no degradation in performance due to heating. A second experiment evaluated the sleeve strainmeter design at elevated pressure. Two strainmeters were evaluated by monitoring strain while they were attached to a standard oil and gas wellbore casing (5.5-inch API) in a custom vessel that was pressurized up to 5000 psi. The strainmeters were functional during the test and calibration data collected after the pressurization were essentially the same as calibration data prior to pressurization, indicating the effects of high pressure were negligible. Reservoir conditions at Utah FORGE are approximately 230°C and 3700 psi. Our experiments demonstrated strainmeter functionality for extended periods at temperatures and pressures significantly greater than those at the Utah FORGE EGS reservoir. The sleeve architecture can accommodate a variety of optical fiber sensors, including fiber Bragg gratings (FBGs), Distributed Acoustic Sensing (DAS) or interferometric sensors, establishing a flexible platform for high-resolution tensor strain measurements in extreme subsurface environments.

1. INTRODUCTION

Enhanced geothermal systems (EGS) extract subsurface energy by maintaining long-term fluid circulation through stimulated fractured rock. Mechanical deformation that occurs during stimulation and production phases provides insight into fracture behavior, permeability changes, stress redistribution, and coupling between the wellbore and the surrounding reservoir (e.g., Rutqvist, 2012). High-resolution borehole tensor strain measurements are therefore desirable to monitor reservoir behavior during stimulation and long-term operations. Borehole tensor strainmeters are available (e.g., Roeloffs, 2010; Murdoch et al, 2023) that can measure multiple strain components with high precision. However, these existing instruments fail in geothermal conditions.

To fill this gap, we developed a tensor strainmeter with a sleeve architecture designed for installation on the outside of well casing. Motivation for this project emerged from interest in measuring strain tensors in the EGS reservoir at the Utah FORGE site. Prototypes were designed and tested in the laboratory. This paper presents two key laboratory evaluations: (1) a high-temperature cyclic loading experiment performed on a composite split-sleeve strainmeter, and (2) a high-pressure qualification test conducted on stainless steel half-sleeve strainmeters. The experiments reported here present new data that build upon previous high-temperature split-sleeve strainmeter testing (i.e., Laffaille et al., 2024), repeating the high-temperature test procedure with strainmeter design modifications and adding a separate high-pressure evaluation.

2. SLEEVE STRAINMETER CONCEPT

The strainmeter design consists of a thin sleeve that couples mechanically to steel well casing using external clamping/banding. Optical fiber strain sensors are embedded within the sleeve to provide directional strain sensitivity while protecting sensing elements. After installation, the casing is grouted in the wellbore annulus, providing mechanical coupling between the strainmeter and formation. The sleeve architecture is adaptable and can host different fiber optic sensing methods. This work focuses on fiber Bragg gratings (FBGs) for laboratory testing due to their availability and multiplexing capability.

Two sleeve designs were evaluated:

1. Composite split-sleeve strainmeter: a fiberglass/resin laminate sleeve that wraps fully around the casing and incorporates a flexible hinge region for installation.
2. Stainless-steel half-sleeve strainmeter: a hermetic stainless-steel shell architecture designed for high-pressure and harsh chemical exposure, with optical fiber elements housed in an internal cavity and bonded using high temperature resin. This design wraps halfway around the casing covering 180 degrees.

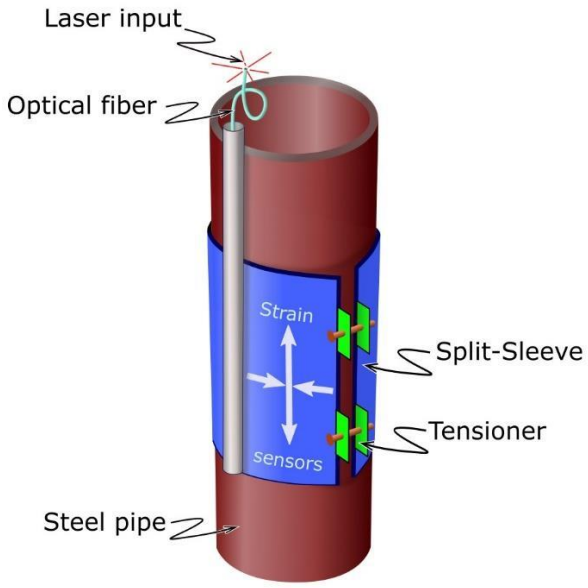

Figure 1: Schematic of a composite split-sleeve strainmeter installed onto borehole casing. Optical fiber is embedded within the composite sleeve and can measure multiple components of strain.

3. HIGH TEMPERATURE PERFORMANCE TESTING

High temperature laboratory experiments were conducted to evaluate the thermal stability and long term reliability of the composite split-sleeve strainmeter.

3.1 Methods

A high-temperature test apparatus applied cyclic transverse loads to evaluate sleeve response at geothermal reservoir temperatures. The apparatus consists of a vertically mounted steel pipe (outside diameter = 2.375 inches) anchored at its base with a centralized heating element in the pipe. The sleeve is mounted onto the pipe and wrapped with insulation. Periodic loading is applied near the top of the pipe (h = 180 cm) using two perpendicular actuators, producing directional bending strains at the sleeve (Figure 2). Pneumatic actuators are regulated with a supply pressure of 28 psig for loading causing ~2.5 mm of displacement at the top of the pipe when extended. The composite sleeve is clamped around the pipe with tensioning bolts and positioned so that sensors were 45 cm above the base of the pipe.

The tests evaluate a split-sleeve strainmeter fabricated using high-temperature resin (Cotronics Duralco 4460, rated to ~315°C) and two embedded FBG strain sensors. The strain sensors consist of polyimide-coated, single-mode silica optical fiber (SMF-28e) with fiber Bragg gratings written in the 1550 nm wavelength band. The two FBGs are oriented parallel to the axis of the sleeve and are denoted as S1 and S2. S1 is positioned with an azimuth of 280° and S2 at 0° (Figure 3). Another FBG (S3) is bonded within a shallow slot in the pipe (S3) to measure axial strain directly and serve as a reference. While clamping the sleeve strainmeter to the pipe, S2 is positioned at the same azimuth (0°) and height (45 cm) as the S3 reference (Figure 3). Incorporating this sensor enables direct comparison between strain measured by the sleeve and true pipe strain during the experiment. 1550 nm FBGs were interrogated with the FAZT I4G interrogator (Femto Sensing International). Over a 60-second baseline-window, strain measured with this interrogator exhibits a standard deviation of 0.05 με.

The loading sequence consists of 60 second loading periods (30 seconds extended, 30 seconds retracted) in a repeated cycle. Actuator A applies nine replicate loads and then another nine loads are applied by Actuator B (Figure 4). For loading cycle A and B, the net strain response was determined for all nine loading events and are averaged. Timing relays are used to repeat this sequence once every three hours.

The strainmeter and pipe were heated in steps starting with 225 °C for 20 days, then 250 °C for 75 days, and 275 °C for 185 days. The strains caused by the loading sequence were measured for nine months. This extended duration test generated data describing the strainmeter response to applied load at high temperatures.

Performance goals for the high temperature tests were:

1. Comparable strain transfer behavior across temperatures ranging from 25 °C to 225 °C
2. Optical functionality of the strainmeter maintained during prolonged exposure at elevated temperature
3. No indications of sensitivity loss during prolonged exposure at elevated temperature

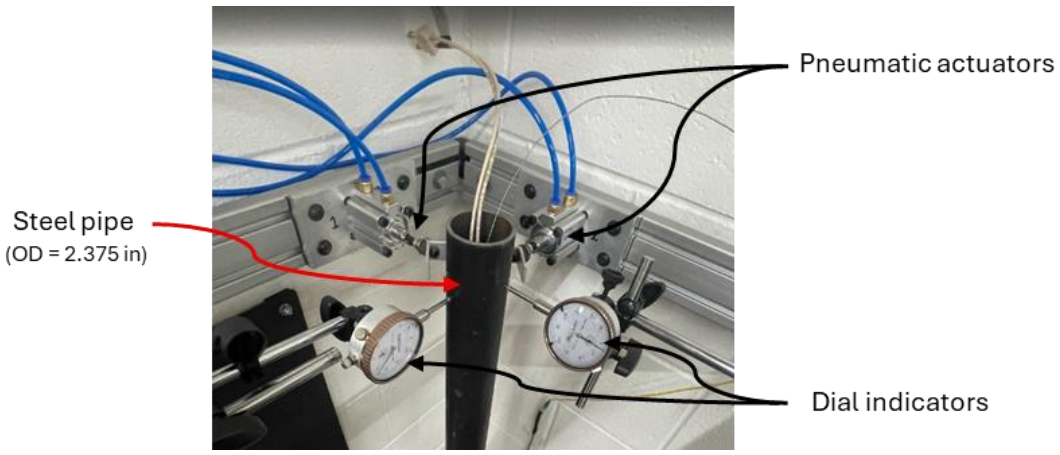

Figure 2: Actuators and upper end of the pipe with an internal heating element used for high temperature performance testing. Dial indicators at top of pipe were used to measure transverse displacement of the pipe

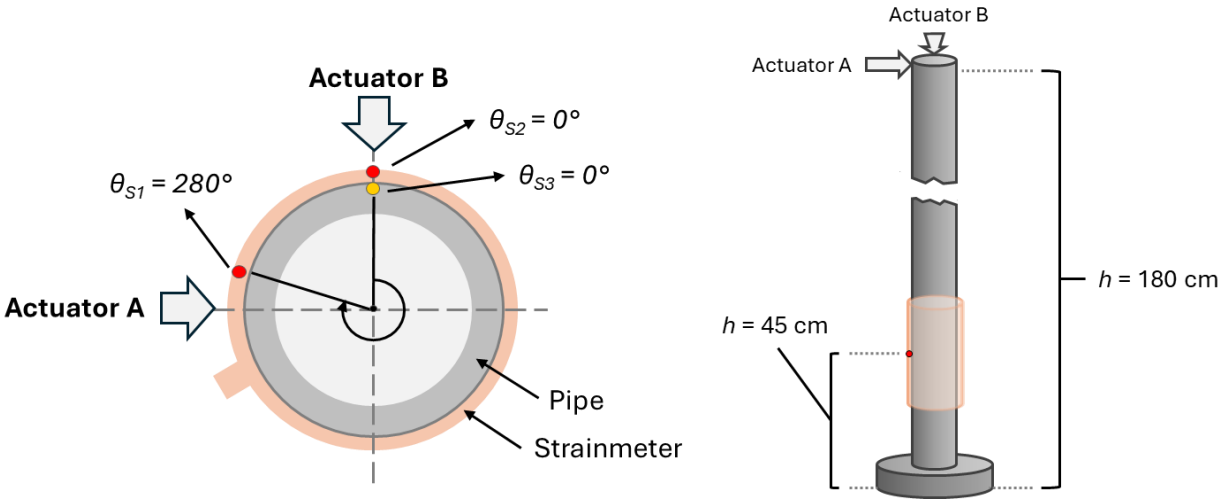

Figure 3: (Left) Top view diagram of the high temperature testing apparatus showing strain sensor azimuths (Θ) relative to their directional loads. (Right) Side view diagram of the high temperature testing apparatus with a sleeve strainmeter mounted to the pipe. Strainmeter sensors (S1, S2) and the pipe embedded sensor (S3) are positioned 45-cm above the base of the pipe and actuators are positioned 180 cm above the base.

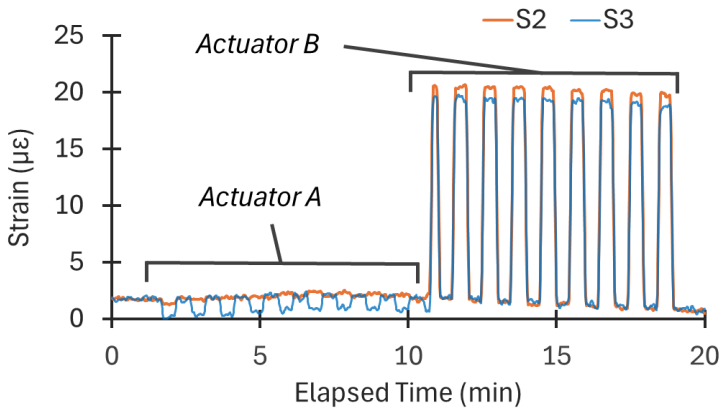

Figure 4: Strain responses from Actuators A and B for a loading cycle completed at 25 °C. Axial strain on the pipe at S3 (blue), and axial strain measured at S2 on the strainmeter (orange).

3.2 Results of High Temperature Tests

High temperature testing results include an evaluation of strain transfer from the pipe to strainmeter, and a review of how the strainmeter performance varied with time while at EGS temperature.

3.2.1 Strain Transfer

A series of controlled bending load tests were conducted to quantify the strain transfer performance of the composite split-sleeve strainmeter over temperatures ranging from 25 °C to 225 °C. In each bending load test, Actuator B applied nine replicate loads to the top of the pipe while strain and pipe displacement were monitored (Figure 3). The tests compared strain measured by the strainmeter (S2) to strain measured on the pipe (S3) to assess the mechanical coupling efficiency as a function of temperature. The strain transfer coefficient (k) was calculated as $k = \Delta\varepsilon_{S2} / \Delta\varepsilon_{S3}$ where $\Delta\varepsilon_{S2}$ and $\Delta\varepsilon_{S3}$ represent the net strain responses of the sleeve-mounted and reference sensors. k values reported in Table 1 are averaged across nine replicate loading events from Actuator B (Figure 4).

Under loading by Actuator B, the strain measured by the strainmeter closely matched both the sign and magnitude of the strain measured on the pipe. At 25 °C, the resulting strain transfer coefficient was $k = 1.04 \pm 0.05$. This coefficient decreased by a few percent with increasing temperature, with measured values $k = 0.95 \pm 0.03$ at 175 °C and $k = 0.94 \pm 0.02$ at 225 °C (Table 1 and Figure 5).

Displacement measured normal to the pipe opposite Actuator B increased from 2.24 mm at 25 °C to 2.62 mm at 225 °C (Table 1) due to increased pipe compliance at elevated temperature. Corresponding increases in axial strain ($\Delta\varepsilon$) were observed at both the S2 (sleeve mounted) and S3 (pipe embedded sensors). Measured and actual strain magnitudes were comparable at all temperatures. Apart from the 135 °C test, k remained between 1.06 and 0.94 across the full temperature range, indicating stable strain transfer performance with increasing temperature. (Table 1).

Table 1: Stain transfer evaluation of a composite split-sleeve strainmeter. Measured $\Delta\varepsilon$ determined from S2 readings, Actual $\Delta\varepsilon$ determined from S3, and strain transfer coefficient (k) determined as $k = \Delta\varepsilon_{S2} / \Delta\varepsilon_{S3}$

Temp. (°C)	*Disp. (mm)*	Measured Δε (με)	Actual Δε (με)	k
25	2.24	18.9 ±0.5	17.8 ±0.4	1.06 ±0.05
100	2.39	17.8 ±0.7	18.5 ±0.7	0.97 ±0.07
135	2.44	17.4 ±1.0	20.2 ±0.3	0.86 ±0.09
175	2.49	20.1 ±0.6	21.3 ±0.2	0.95 ±0.03
200	2.54	19.6 ±0.3	20.9 ±0.3	0.94 ±0.02
225	2.62	21.6 ±0.2	23.0 ±0.4	0.94 ±0.02

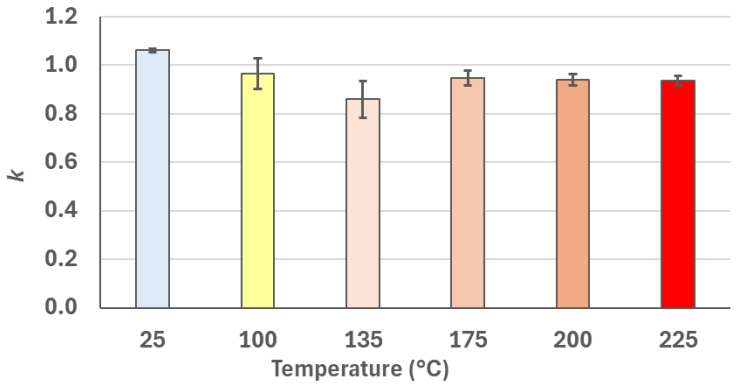

Figure 5: Strain transfer coefficients (k) as function of temperature where $k = \Delta\varepsilon_{S2} / \Delta\varepsilon_{S3}$

3.2.2 Extended Duration Test

The extended duration experiment was conducted as a single continuous test, with the apparatus held at successively higher temperatures during stepped phases. The apparatus temperature was held at 225 °C for approximately three weeks, 250 °C for the following 75 days, and 275 °C for 185 days. Loading sequences, occurring once every three hours, were used to evaluate changes in strainmeter response across this test.

The strain response to applied load at S3 (the pipe reference), was essentially the same as the response at S2 (the strainmeter), during the first 90 days of testing (Figure 6). Connection with S3 was lost after 90 days, but S1 and S2 in the sleeve strainmeter remained functional and continued to produce consistent responses throughout the duration of the experiment. The average difference between the measured

(S2) and true strain (S3) across the first 90 days was 3.3 ± 2.1 με for Load B. This is an average strain transfer coefficient of k = 0.86 ± 0.08.

The response to applied load drifted subtly with time, but no systematic change was correlated with the duration or magnitude of temperature. In general, the experiment demonstrated a consistent response to applied load at or above 225 °C for more than five months, showing that the composite split-sleeve strainmeter can maintain strain response stability at geothermal reservoir temperatures for long periods.

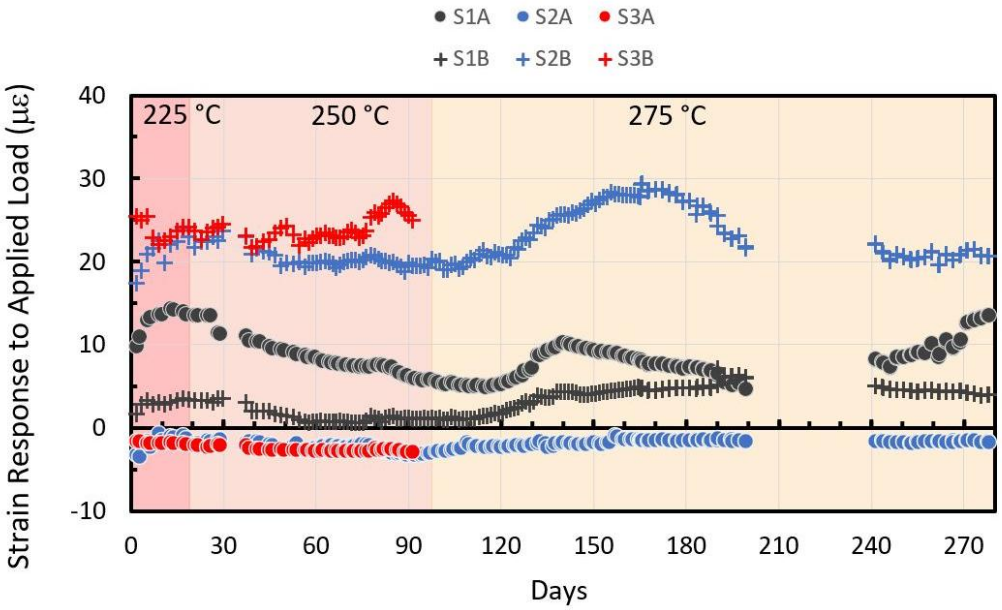

Figure 6: Measured strain response (με) of a composite split-sleeve strainmeter subjected to axial loading events while exposed to reservoir temperatures for 280 days. The sleeve strainmeter contains two FBG sensors (S1 and S2). True axial strain was evaluated by an additional FBG sensor (S3) embedded in the pipe. A and B sensor notations correspond to directional loads from Actuator A and Actuator B

4. HIGH PRESSURE TESTS

The stainless-steel half-sleeve strainmeter design was tested at elevated pressures to evaluate the potential for failure at reservoir pressures.

4.1 Methods

Two stainless-steel half-sleeve strainmeters were evaluated using a hydrostatic pressure vessel rated for 10,000 psi at the University of Oklahoma. Both strainmeters contained two 850 nm FBGs oriented circumferentially within the metal shell and were interrogated with the FiSpec X100 (FiSens GmbH). The strainmeters were designed to clamp around a 5.5-inch API steel casing tensioned with Band-it straps (Figure 8).

The pressure vessel was fabricated from a 7-ft-long thick-walled steel pressure tube with an internal diameter of 7-inches and an outer diameter of 11 inches. The vessel provided an internal test volume approximately 84-inches in length and was designed for safe testing of at least at least 10,000 psi internal pressure (Figure 7). The maximum operating pressure during testing was limited by the pressure rating of the installed compression fittings and feedthrough hardware rather than the vessel body. Custom steel end caps were fabricated to accommodate optical fiber feedthroughs to allow strain monitoring during pressurization. Fluid pressure was controlled by a piston pump plumbed to the vessel.

Performance goals for the pressure test were:

1. Optical functionality maintained during pressurization
2. Comparable calibration behavior before and after high pressure exposure

Calibration testing utilized a custom built radial loading apparatus designed to apply internal diameter (ID) loads at controlled angular orientations in a lab setting (Figure 9). Calibration was performed by applying radial loads at 5° angular steps across a 180° range.

The first high-pressure test was conducted by sealing the strainmeter in the vessel and stepping the pressure up to 2000 psi and then 5000 psi and holding it at 5000 psi for roughly 1-hr. The optical fiber from the strainmeter was routed to an optical interrogator and the strain was measured throughout the test. The second test used the other strainmeter and it involved ramping the pressure up to 5000 psi and leaving the apparatus at pressure overnight for a total exposure time of 13-hours. The strainmeter was removed the next day and recalibrated after traveling back to Clemson.

Figure 7: High pressure testing apparatus at University of Oklahoma configured to evaluate functionality of prototype sleeve strainmeters at Utah FORGE reservoir pressures.

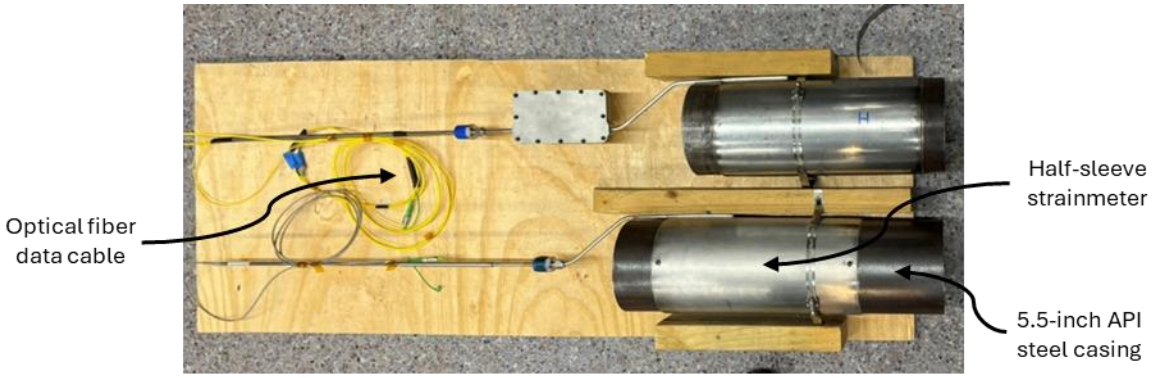

Figure 8: Two stainless-steel half-sleeve strainmeters prepared for high pressure testing. Instrument ID: SS-2-625 (Bottom), Instrument ID: S-SS-2-425; Instrument ID: SS-2-825 (Top)

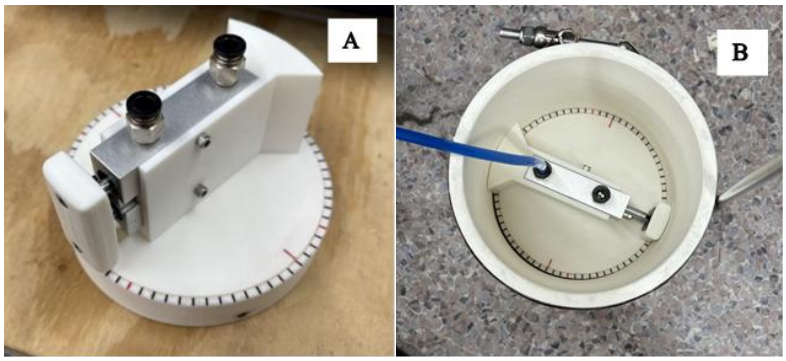

Figure 9: (A) Radial loading device custom built for calibrating stainless steel half-sleeve strainmeter. (B) Top view of device looking down inside a casing.

4.2 Results of High Pressure Tests

Both half-sleeve strainmeters remained functional throughout pressurization to 5000 psi. The vessel was filled with water for the first 50 minutes of the test and then pressure was ramped to 2000 psi for 30 minutes and then increased to 5000 psi and for a full hour. The strain response increased with pressure by 50–100 με at one sensor and 150–300 με at the other one (Figure 10).

In the second high-pressure test, the strain increased by approximately 150 με during the initial increase to 5000 psi and then decreased roughly linearly to approximately -150 με 12 hours later. (Figure 11).

The tensile strain observed during the tests was surprising because we expected an increase in pressure to cause compression. One explanation is that the tensile strain is a thermoelastic effect resulting from Joule-Thompson heating during pressurization. Using the Joule–Thomson coefficient for water (0.2–0.5°C/MPa), a pressure increase of 5000 psi (~34 MPa) would produce 7–17°C temperature increase. This would cause a thermoelastic strain in 304 stainless-steel of approximately ~120–290 με, consistent with the strain change during pressurization. The strain decrease during the second test (Figure 1) likely occurred due to cooling of the pressure vessel overnight (it was in a storage container without temperature regulation).

After pressure testing, both strainmeters appeared essentially the same as they did prior to exposure—they were undamaged by the high pressure. The circumferential strain at the FBGs during calibration testing (Figure 9) was approximately a sinusoidal function of orientation with an amplitude of 2 to 3 με prior to pressure testing (Figure 12). Data from calibration tests after pressure testing is essentially the same as the initial test (Figure 12).

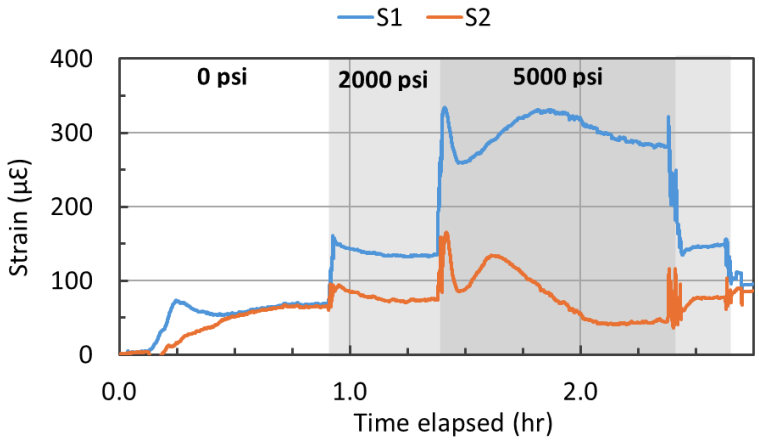

Figure 10: Strain time-series recorded during high pressure test #1. Strain measured by a stainless-steel half-sleeve strainmeter while sealed inside a pressure vessel. Hydrostatic loading occurred at an elapsed time of 0.9 hours (2000 psi) and at 1.4 hours (5000 psi). The internal pressure of the vessel was fully released at an elapsed time of 2.6 hours.

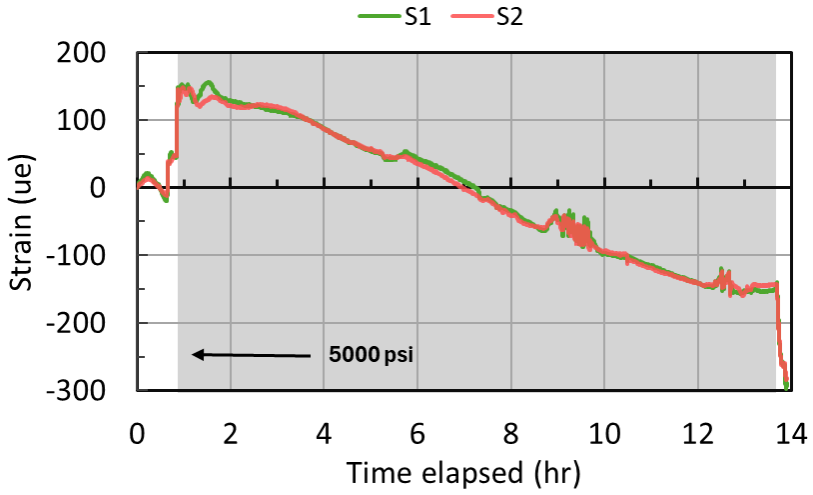

Figure 11: Strain time-series recorded during high pressure test #2. Strain measured by a stainless steel half sleeve strainmeter during an overnight high pressure test. Hydrostatic loading occurred at an elapsed time of 0.8 hours (5000 psi) and was released at 13.4 hours

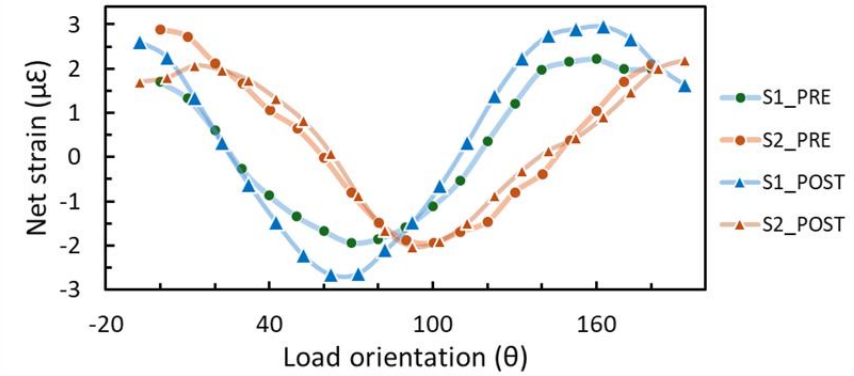

Figure 12: Comparison of radial load calibrations completed before and after high pressure testing (Instrument ID: S-SS-2-625). Plots show net strain response (με) to loading with respect to load orientation.

5. DISCUSSION

The results of the laboratory tests indicate that the sleeve architecture can be used to create tensor strainmeters that can function under pressure and temperature conditions of EGS reservoirs. The sleeve architecture is important for this application because it can be deployed in the annulus between the outside of casing and the borehole wall. The sleeve itself is less than 2.5 mm thick, and it includes a housing that is less than 10 mm, which should be accommodated in the annular space of most completions. The design requires an optical fiber to extend from the instrument through the annular space to an interrogator at the ground surface, but this type of deployment of optical fiber is widely used for DAS applications.

The tests reported here used a split-sleeve design to demonstrate performance at high-temperature and a half-sleeve design to demonstrate performance at high-pressure. The split-sleeve design was developed to create an instrument that wraps entirely around the casing because this geometry is ideal for measuring multiple components of strain required to characterize the strain tensor. That design uses composite materials with a flexible axial band that allows it to open when it is fit around the casing. The composite materials function well at high temperature, but we were concerned that they might have problems at high-pressure. That motivated us to develop the half-sleeve design, which has an entire external shell of stainless-steel and functions at high pressure. The half-sleeve design covers half the circumference of the casing, so it has a smaller 3D extent than the split-sleeve, but it still has good resolution of the strain components normal to the axis of the casing. The half-sleeve design was not tested at high-temperature during this study because of time constraints, but the materials and key fabrication methods are based on the split-sleeve design, so we are confident that it will perform at high-temperature much like the split-sleeve design.

The sleeve architecture is designed to be used with a variety of optical fiber sensing techniques. We used FBGs and we evaluated at high temperature optical fiber Mach-Zehnder sensor, but the configuration could also be used to give 3D sensing capabilities to DAS or DSS sensing methods. We envision applications where multiple sleeves are integrated with DAS to provide 3D strain measurements as a sparse array along the continuous uniaxial measurements from DAS. The results from the laboratory tests indicate that this application should not be limited by the high temperature and pressures of EGS reservoirs.

6. CONCLUSION

Laboratory evaluations demonstrate that tensor strainmeter with sleeve architectures can operate under geothermal reservoir conditions:

1. Mechanical coupling of the composite split-sleeve strainmeter remains effectively temperature independent between 25 °C and 225 °C with respective k values marginally decreasing from 1.06 ± 0.05 to 0.94 ± 0.02
2. A composite split-sleeve strainmeter produced stable strain responses to loading at 225–275°C for 280 days with no indication of systemic sensitivity loss
3. Two stainless-steel half-sleeve strainmeters remained operational during a 1-hour and 12-hour exposure to 5000 psi. Pre- and post-calibration responses were essentially unchanged, indicating that those pressures should not limit downhole applications.

Reservoir temperature and pressures at Utah FORGE (230 °C, ~3700 psi) are below the maximum evaluated in this study, providing a margin for deployment. Together, the high-temperature and high pressure test results demonstrate that sleeve based strainmeter designs can tolerate the combined thermal and pressure conditions expected in EGS reservoirs.

7. ACKNOWLEDGEMENT

The authors gratefully acknowledge support from the U.S. Department of Energy under Grant No. DE-EE0007080-3-2514, *Enhanced Geothermal System Concept Testing and Development at the Milford City, Utah FORGE Site*, and Grant No. DE-EE0007080-1-2410, *Development of a Smart Completion & Stimulation Solution.*

REFERENCES

Laffaille, C., Parris, J., DeWolf, S., Germanovich, L., and Murdoch, L. C.: Feasibility of Measuring the Strain Tensor at Geothermal Reservoir Temperatures, Proceedings, *49th Workshop on Geothermal Reservoir Engineering*, Stanford University, Stanford, CA (2024).

Murdoch, L. C., DeWolf, S., Germanovich, L. N., Moysey, S., Hanna, A., Roudini, S., & Moak, R.: Using the shallow strain tensor to characterize deep geologic reservoirs, *Water Resources Research*, 59, OSTI ID: 1923717 (2023).

Roeloffs, E. A.: Tidal calibration of Plate Boundary Observatory borehole strainmeters: Roles of vertical and shear coupling, *Journal of Geophysical Research: Solid Earth*, 115, B06405 (2010).

Rutqvist, J.: The geomechanics of CO_2 storage in deep sedimentary formations, *Geotechnical and Geological Engineering*, 30, 525-551 (2012).